Organic–inorganic hybrid titanophosphite proton conductive membranes with graded monomer conversion

AUTHOR(S):

Tokuda, Yomei; Nishioka, Satoshi; Ueda, Yoshikatsu; Koyanaka, Hideki; Masai, Hirokazu; Takahashi, Masahide; Yoko, Toshinobu

CITATION:

Tokuda, Yomei ...[et al]. Organic–inorganic hybrid titanophosphite proton conductive membranes with graded monomer conversion. Solid State Ionics 2012, 206: 22-27

ISSUE DATE:

2012-01

URL:

http://hdl.handle.net/2433/152382

Organic-inorganic hybrid titanophosphite proton conductive membranes with graded monomer conversion

Yomei Tokuda[a,*], Satoshi Nishioka[a], Yoshikatsu Ueda[b], Hideki Koyanaka[c], Hirokazu Masai[a], Masahide Takahashi[a,d], and Toshinobu Yoko[a]

[a]Institute for Chemical Research, Kyoto University, Gokasho, Uji, Kyoto 611-0011, Japan

[b]Institute for Sustainable Humanosphere, Kyoto University, Gokasho, Uji, Kyoto 611-0011, Japan

[c]Institute for Integrated Cell-Material Sciences, Kyoto University, Yoshida Ushinomiya-cho, Sakyo-ku, Kyoto 606-8501, Japan

[d]Present affiliation: Graduate School of Materials Science, Osaka Prefecture University, Gakuencho 1-1, Naka-ku, Sakai, Osaka 599-8531, Japan

*Corresponding author

E-mail: tokuda@noncry.kuicr.kyoto-u.ac.jp

Institute for Chemical Research, Kyoto University, Gokasho, Uji, Kyoto 611-0011, Japan

Tel:+81-774-38-4721

Fax:+81-774-33-5212

Abstract

Further advances in polymer electrolyte fuel cells require membranes that can operate at intermediate temperatures between 100 and 150 °C. In this study, we report a unique organic–inorganic hybrid titanophosphite membrane possessing high proton conductivity at such intermediate temperatures. The membrane was prepared to have a graded monomer conversion from its surface to its inner parts, by ultraviolet light (UV) absorption of titanate during UV-initiated photopolymerization. The surface of the membrane was completely polymerized to be water durable, whereas its inner parts were weakly polymerized, thus allowing VPA to function as a proton donor. This gives proton conductivities that are as high as 6.3×10^{-4} S cm^{-1} at 130 °C under a dry atmosphere.

Keywords: organic-inorganic hybrid membrane, proton conductor, monomer conversion, polymerization control

1. Introduction

Future advances in fuel cell technology are contingent on the development of new materials. One such material is the Nafion® membrane (DuPont, Wilmington, DE, USA); it is a proton-conducting membrane and has been employed in polymer electrolyte fuel cells (PEFCs). However, the PEFC faces problems including poor carbon monoxide tolerance and heat rejection in temperatures between 60 and 80 °C. In order to overcome these drawbacks, a proton-conducting membrane is required to operate at intermediate temperatures around 100–150 °C [1] and should possess good durability and thermal stability. However, the proton conductivity of Nafion is reported to be low at such intermediate temperatures because proton conduction in Nafion requires the presence of water [2] and the density of acidic sites is as low as 0.9 mmol/g [3- 9].

To solve the abovementioned problems, membranes of polyvinylphosphonic acid (PVPA) have been proposed [3]. The proton conductivity of PVPA membranes at intermediate temperatures is higher than that of Nafion because of the higher number of acidic sites present in PVPA. Accordingly, several types of PVPA-related membranes have been developed; however, these membranes are not water durable [10]. Copolymerization with hydrophobic monomers has been attempted to enhance

the water durability of such membranes [11]. Unfortunately, copolymerization with a hydrophobic monomer substantially decreases the concentration of acidic sites, i.e., -POH, leading to a decrease in the proton conductivity.

In this study, we describe a novel technique to prepare a membrane with a graded monomer conversion using ultraviolet light (UV) irradiation during radical photopolymerization. A schematic procedure is shown in Fig. 1. High conversion at the surface of the membrane enhanced durability while low conversion at the inner part of the membrane facilitated proton conductivity. This incremental change in the proton conductivity is possible because pK_{a1} of vinylphosphonic acid (VPA) is 2.74 and pK_{a2} is 7.34 [12], while pK_a of PVPA is around 5–6. Copolymerization of VPA with an additive monomer of hydrophobic nature having a low chain transfer constant leads to an increase in the conversion of the additive polymer. This procedure produces a PVPA-additive copolymer having high conversion at the surface, whereas the additive polymer in the inner part has low conversion of PVPA. Thus, the membrane consists of a shell made of a PVPA-additive copolymer for blocking moisture and a core of high proton density.

Recently, we have proposed solvent-free reactions for preparing organic-inorganic hybrid materials using orthophosphoric acid and organically modified silanes

[13, 14]. In a solvent-free reaction, the following metathesis occurs on heating: M–X + P–OH → M–O–P + HX↑ (X = Cl, ethoxy). Groups that do not participate in this reaction are omitted from the reaction formula. Because of the absence of solvent evaporation, a crack-free monolith can be produced by simply mixing the starting reagents followed by post baking. Additionally, a product prepared by metathesis uniformly contains an almost complete alternating copolymer of oxide in the form of M–O–P. The above technique can be employed if UV-absorbable oxides such as titanophosphite are incorporated into the copolymer; the intensity of UV light during photopolymerization decreases as the penetration depth increases [15], according to the Beer-Lambert law. Gradation of monomer conversion occurs along the depth of the membrane.

In this study, titanium tetraisopropoxide (TTIP) and ethylmethacrylate (EMA) were selected as the alkoxide and additive monomer starting materials, respectively. Because of the low chain transfer constant of EMA, the EMA radical is expected to be sufficiently stable to promote a large conversion. In addition, EMA was also used as a diluent to decrease the reactivity between TTIP and VPA. Furthermore, water durability is improved because of the hydrophobic nature of polyethylmethacrylate (PEMA).

NMR spectroscopy was employed to confirm the structure and the graded monomer conversion of the membrane. Thermal and chemical stabilities of the membrane were assessed and the proton conductivity was determined.

2. Experimental

2.1 Sample preparation

Four types of membrane were prepared in this study. Vinylphosphonic acid (VPA), TTIP, and a polymerization initiator, Irgacure 1700, were used as received. EMA was purified by stirring in 1 M NaOH solution to remove a polymerization inhibitor. TTIP was first diluted with EMA to avoid any rapid reaction with VPA. The mixture was then added to VPA at 50 °C under N_2 atmosphere and stirred for 90 min to afford a precursor liquid. Irgacure 1700 (1.0 wt%) was added to the precursor. The resulting mixture was poured into a polydimethylsiloxane mold (diameter 10 mm, thickness 1 mm). The mixture was irradiated from both sides using a high-pressure mercury lamp (UI-501C, Ushio, Tokyo, Japan) for 2 h at 50 mW/cm^2 to afford the membranes (VET). Additionally, VET was further heat-treated (VET-ht) as shown in Fig. 2. Membranes of VPA–EMA copolymer (VE) and polyvinylphosphonic acid (PVPA) were also prepared for comparison, following the procedure described for

VET. Thus, VPA and/or EMA was stirred at 50 °C for 90 min and irradiated with UV light following the addition of Irgacure 1700. The four types of membrane prepared are listed in Table 1. Monoliths with thickness of 5 mm were also prepared by irradiating one of the two sides for 1 h to confirm polymerization gradation.

2.2 Analyses of the local structure and the monomer conversion in the membrane

Structural analyses were performed using an NMR spectrometer (JEOL, CMX 400, Tokyo, Japan). The 90° pulse and the delay time were 3 μs and 10 s, respectively. ^{31}P MAS NMR spectra were obtained at a spinning rate of 10 kHz for solid-state analysis of the membranes. Chemical shifts are expressed in parts per million (ppm) with respect to phosphoric acid (0 ppm). In order to confirm the conversion gradation, ^{31}P MAS NMR spectra for irradiated and non-irradiated sides of a 5-mm-thick monolith were also acquired.

Fourier transformed infrared spectroscopy (FT-IR, Thermo Nicolet Avatar 360, Thermo Nicolet, Madison, WI, USA) using the KBr pellet method was employed; a mixture of the membrane (2 mg) and KBr (250 mg) was ground using a pestle and mortar and pressed under a pressure of 60 MPa for 15 min to afford a KBr pellet.

2.3 Characterization of the thermal stability, water durability, and conductive property of membranes

Thermal stability was characterized by thermogravimetry (TG, Rigaku TG 8120, Rigaku, Tokyo, Japan) with a heating rate of 5 °C/min.

Phosphorus (P) elution analysis was also performed to confirm the water durability of the membrane. The sample (diameter 10 mm, thickness 1 mm) was soaked in 350 mL of distilled water at 22 °C with stirring. 2 mL of the solution was extracted at several time intervals (1 min, 5 min, 10 min, 30 min, 60 min, 2 h, 6 h, 20 h, and 48 h). Inductively coupled plasma atomic emission spectroscopy (ICP-AES, Shimadzu, ICPS-8000) was performed on the extracted solutions, with a dilution ratio of 1/500.

For electrical conductivity measurements, the samples were coated with an electrically conductive adhesive (SILBEST® No. 8560) on both the sides, and a Pt wire was used as an electrically conductive lead. The electrical conductivity was measured perpendicular to the membrane by frequency response analysis of the alternating current (AC) impedance spectra (Solartron 1255B and SI 1287, AMETEK, Hampshire, UK). The applied amplitude and AC frequency range were 100 mV and 1 mHz–1 MHz, respectively. To characterize the proton conductivity

under a dry atmosphere, the membrane was first dried under reduced pressure for 24 h, and the conductivity was recorded under N_2 atmosphere. When the temperature was changed, the conductivity was recorded once a constant conductivity value was reached.

3. Results

3.1 Appearance of membranes

The precursor liquids used to fabricate the four types of membranes were viscous, homogeneous, and yellow in color. The final products, i.e., VET-ht obtained after UV irradiation and additional heat treatment, were transparent, homogeneous, yellow, crack-free, and water-durable (Fig. 3).

3.2 Local structure of precursor liquids and membranes characterized by ^{31}P NMR spectroscopy

The precursors and hybrids exhibited several types of bonding, such as P–O–H, P–O–P, and P–O–Ti. In this context, the following abbreviations were used: T^n(X) refers to $P(OX)_n$ bonds, where X = P or Ti; T^n*(X) denotes phosphorus in PVPA with $P(OX)_n$ bonds, where the symbol * denotes the polymerization of the vinyl group.

The term polymerization refers to polymerization between organic monomers, while polycondensation describes alcohol condensation between VPA and TTIP or the dehydration condensation of VPA.

^{31}P NMR spectra of the precursor solutions are shown in Fig. 4. As previously reported [13, 9], the peaks around 17–18 ppm can be assigned to T^0 of VPA. The solvation effect in the precursors was also observed, as evidenced by the high-field shift of T^0 from VPA [14]. The presence of a single peak in VE and PVPA precursors indicated that the polycondensation of the -POH groups did not occur below 50 °C. In contrast, the spectrum of VET precursor exhibited three peaks, indicating that condensation between VPA and TTIP occurred to produce P-O-Ti bonds. Thus, the peaks at 12.2 and 7.2 ppm were attributed to T^1(Ti) and T^2(Ti, Ti), respectively.

^{31}P MAS NMR spectra of the membranes VET, VET-ht, VE, and PVPA are shown in Fig. 5. All the spectra were normalized. The total area is proportional to the amount of VPA used. Peaks around 17 and 12.2 ppm were assigned to T^0 and T^1(Ti), respectively. As previously reported [16], the peak around 30.0–38.0 ppm can be attributed to polymerized VPA, T^0*. A comparison between the spectra of VET and VET-ht showed that the peak assigned to T^0* decreased, while there was an increase in the intensity of the broad peak around 23–26 ppm. Because the POH

moieties in PVPA condensed to form P-O-P bonds during heat treatment, the broad peak observed in VET-ht around 23–26 ppm can be attributed to T^1*(P).

^{31}P MAS NMR spectra for UV-irradiated and non-irradiated sides of a 5-mm-thick monolith are shown in Fig. 6. On the basis of the assignments made above, it can be seen that the intensity of T^0 is less whereas T^0* has a greater intensity in the irradiated side of the monolith than in the non-irradiated side.

3.3 Local structure of the precursor liquids and membranes characterized by FT-IR spectroscopy

FT-IR spectra of the starting reagents and the membranes are shown in Fig. 7. The peaks observed at 1726–1718, 1694–1683, 1640, and 1407 cm^{-1} correspond to the stretching modes of the ketone in EMA, the stretching modes of the ketone in EMA combined with POH, the vinyl group in EMA, and the vinyl group in VPA, respectively [17,18,19]. The stretching mode of the vinyl group of EMA at 1640 cm^{-1} almost disappeared in all the membranes, while the strong absorbance of the vinyl group of VPA can be observed in VET, and VET-ht and to a lesser extent in VE. These results indicated that EMA in all the membranes has polymerized, however; VPA still remains in VET and VET-ht.

3.4 Thermal stability of membranes

TG-DTA curves of the membranes are shown in Fig. 8. Weight losses over the ranges 100–160, 160–270, and 280–350 °C were due to water evaporation, condensation of -POH, and oxidation of organic chains, respectively. VET-ht was thermally stable up to 200 °C because of the elimination of water and residual POH groups by post-heat treatment of VET.

3.5 Assessment of water durability of membrane by phosphorous elution analysis

PVPA was completely dissolved in water after being immersed for 30 min as reported [10], while VE, VET, and VET-ht retained their appearance after 24 h. The eluted fraction of P was plotted against the square root of time (Fig. 9). The slopes of the plots were in the following order: VET < VET-ht < VE << PVPA. The slopes of the plots showed that VET and VET-ht were five times more durable than PVPA. VET-ht is less durable than VET owing to crack formation that occurs on heat treatment. Thus, the heat-treatment process needs to be further improved. The durability was found to be in the following order: VET > VET-ht > VE >> PVPA,

which indicates that copolymerization with organic-inorganic hybridization improves the durability of the membrane.

3.6 Proton conductivity of the developed membrane

Arrhenius plots of the proton conductivities of the developed membrane and Nafion under nitrogen atmosphere are shown in Fig. 10. The proton conductivity of the developed membrane was higher than that of Nafion because Nafion requires sufficient humidification for proton conductivity [2]. Additionally, the proton conductivity of VE, VET, and PVPA is non-linear above 80 °C owing to condensation of -POH while that of VET-ht increased below 150 °C. The proton conductivity of VET-ht was evaluated to be 6.3×10^{-4} at 150 °C and 1.1×10^{-5} at 80 °C under N_2 atmosphere.

4. Discussion

4.1 Reaction mechanism during precursor formation

We first focus on polycondensation during heating to obtain precursor VET. From the starting composition of VET (VPA:TTIP = 95:5), it is found that the ratio of the number of -POH in VPA to the isopropoxy groups in TTIP is 190:20. Assuming that

all the isopropoxy groups react with hydroxyl groups in -POH, we can conclude that 10.5% of hydroxyl groups in -POH are consumed. From the ^{31}P NMR spectra shown in Fig. 4, we can calculate the areas of T^0, T^1(Ti), and T^2(TiTi) to 81.5, 14.5, and 3.8%, respectively. The percentage of -POH groups that reacted with TTIP can be calculated as (14.5 × 1 + 3.8)/2 = 11.1 (%), where division by two is necessary because each VPA unit possesses two POH groups. The calculated value is almost equal to the assumed consumption percentage of 10.5 %. This result indicates that almost all of TTIP reacted with VPA. Therefore, the following metathesis (alcohol condensation) is proposed to occur during heating:

$$POH + TiO^iPr \rightarrow P\text{-}O\text{-}Ti + HO^iPr\uparrow,$$

while the dehydration condensation of VPA does not occur. Thus, a simple mixing and heating of VPA and TTIP diluted with EMA provides an inorganic alternating copolymerization structure, Ti-O-P, without any side reactions.

We now discuss the local structure of P in the membrane obtained by photopolymerization. The normalized areas of the peaks in the ^{31}P MAS NMR spectra shown in Fig. 5 are tabulated in Table 2. Obviously, Ti-O-P structure, T^1(Ti), still remains in membranes VET and VET-ht. It is noted that the amounts of T^0 and VPA monomer in VET and VET-ht were greater than those in VE and PVPA. This is

attributed to the incorporation of TTIP, which will be discussed later. As compared to the amounts of T^{0}* and T^{1}*(P) in VET, the amounts of T^{0}* decreased and T^{1}*(P) increased in VET-ht, which was heat-treated, indicating that polymerization of the vinyl group of phosphite proceeds during heating. In addition, the decrease in T^{0} indicated the formation of P-O-P bonds by condensation of -POH. It was found that both polymerization and condensation had occurred in VET-ht during post heating of VET, whereas the VPA monomer still remained in the VET-ht membrane.

4.2 Monomer conversion in the membrane after UV irradiation

The ^{31}P MAS NMR spectra of the 5-mm-thick membrane cut into two pieces support the abovementioned conclusion that VPA still remains in the membrane. The peak area assigned to monomeric VPA of the non-irradiated side was more than that of the irradiated side, while the peak area corresponding to polymeric VPA of the non-irradiated side was smaller than that of the irradiated side. As well known, titanium absorbs UV light, although its band edge depends on a ligand. Previously, we have made the buckling structure on a thin film by means of the UV absorption due to titanium [15]. In that case, the penetration depth of the UV light became to be so short that the UV-irradiated side was polymerized while non-irradiated side

not well. Although the concentration of titanium in the present experiment is less than that in the previous one, thickness in the membrane VET is larger than the thin film. Therefore, the intensity of UV light at the inner part is expected to be low enough to suppress the polymerization. Thus, it is concluded that titanium produces the gradation of the the monomer conversion in the membrane in spite of low concentration of titanium in the precursor VET. The detailed analysis using UV-vis spectroscopy was also shown in ref. 20. The existence of absorption of VPA in FT-IR spectra (Fig. 7) also indicated that a part of VPA remains inside the membrane because the membrane was exposed by UV light from their both sides.

Although the exact conversion gradation in the present membrane has not been determined, it is considered that (1) monomer conversion becomes saturated up to a certain point from the surface because UV exposure times can be as long as 2 h, (2) the conversion starts to decrease at a certain point, (3) the conversion reaches a minimum at the core of the membrane.

4.3 Proton conductivity of membranes

Proton conductivity of membranes VET, VE, and PVPA became non-linear around 100 °C while that of VET-ht was linear over 100 °C. As already discussed,

water evaporation can be observed between 100 and 160 °C, which serves to explain the non-linearity.

The proton conductivity of VET-ht is linearly dependant on 1/T. Therefore, the activation energy E_a can be expressed as follows:

$$\ln \sigma = \ln A - E_a/\mathrm{R}T, \quad (1)$$

where σ, A, and R are the electrical conductivity, frequency factor, and gas constant, respectively. The activation energies for the present hybrids were calculated as ~74 kJ/mol. This value indicates that proton conduction is similar to the Grotthuss mechanism [2], where the protons are hopping between adjacent -POH groups.

Additionally, the conductivities of both the VET and VET-ht membranes were higher than that of VE. The residual VPA acts as a proton donor. Simple mixing of VPA with a hydrophobic monomer, as shown in VE, is not beneficial for achieving water durability because of the decrease in the acidic sites. In this study, water durability is enhanced when compared to PVPA by means of high monomer conversion at the surface and copolymerization with a hydrophobic monomer. On the other hand, VET-ht exhibits a proton conductivity of 6.3×10^{-4} Scm^{-1} at 150 °C under N_2 atmosphere because of the residual VPA in the inner part. For practical applications, the proton conductivity of the VET-ht will be higher than that

reported since humidification is performed to some extent. Indeed, as reported, the proton conductivity of VET-ht was 8.0×10^{-4} at 80 °C and 85 %RH, which was 72 times higher than that measured under N_2 atmosphere [20]. Thus, the preparatory technique proposed in this study is useful for the fabrication of a proton conductor at intermediate temperatures. The present VET-ht membrane is a potential candidate for a highly proton-conductive membrane having good thermal stability.

5. Conclusion

We have developed a membrane possessing graded monomer conversion from its surface to its inner parts using UV absorption of titanate during photopolymerization, as shown in the case of poly(vinyl phosphonic acid-co-ethyl methacrylate) copolymer combined with titanate, VET-ht; the high conversion at the surface is effective for enhancing water durability while the low conversion in the inner part of the membrane facilitates high proton conductivity. The proton conductivity of the VET-ht membrane was 6.3×10^{-4} Scm^{-1} at 150 °C even under dry conditions. The durability of the membrane VET-ht was much higher than that of polyvinylphosphonic acid, PVPA. The membrane was also thermally stable up to 200 °C. These properties contribute to overcome the conventional problems

associated with decreases in proton conductivity of polymer electrolytes at intermediate temperatures between 100 and 150 °C.

Tables and figures captions

Table 1 Sample notation and composition

Table 2 Normalized area of the peaks in ^{31}P MAS NMR spectra of hybrid membranes

Fig. 1 Schematic representation of membrane possessing graded degrees of polymerization: (a) titanophosphite precursor, (b) copolymerized membrane having graded degrees of polymerization

Fig. 2 Temperature program of heat treatment

Fig. 3 Photographs of samples prepared

Fig. 4 ^{31}P NMR spectra of VET, VE, and PVPA precursor solutions

Fig. 5 ^{31}P MAS NMR spectra of various hybrid membranes

Fig. 6 ^{31}P MAS NMR spectra of thick VET membrane. Black and red lines indicate the spectra of UV-irradiated side and non-irradiated side, respectively.

Fig. 7 FT-IR spectra of several hybrid membranes (VET, VET-ht, VE)

Fig. 8 TG-DTA curves of various hybrid membranes

Fig. 9 Time dependence of eluted P recorded by ICP optical emission spectrometry

Fig. 10 Temperature dependence of proton conductivity in the absence of humidification

Acknowledgment

This work was financially supported by a Grant-in-Aid for Scientific Research, No. 20613007 and Exploratory Research for Sustainable Humanosphere Science, Kyoto University. One of the authors (Y. T.) acknowledges financial support from The Murata Science Foundation.

[1] K.D. Kreuer, J. Membr. Sci. 185 (2001) 29–39; J.A. Kerres, J. Membr. Sci. 185 (2001) 3–27.
[2] K. D. Kreuer, S. J. Paddison, E. Spohr, M. Schuster, Chem. Rev. 104 (2004) 4637–4678.
[3] H. Steininger, M. Schuster, K. D. Kreuer, A. Kaltbeitzel, B. Bingol, W. H. Meyer, S. Schauff, G. Brunklaus, J. Maier, H. W. Spiess, Phys. Chem. Chem. Phys. 9 (2007) 1764–1733.
[4] R. P. Pereira, M. I. Felisberti, A. M. Rocco, Polymer 47 (2006) 1414–1422.
[5] F. Sevil, A. Bozkurt, J. Phys. Chem. Solids 65 (2004) 1659–1662.
[6] H. Erdemi, A. Bozkurt, Eur. Polym. J. 40 (2004) 1925–1929.
[7] J. Parvole, P. Jannasch, Macromolecules 41 (2008) 3893–3903.
[8] M. Yamada, I. Honma, Polymer 46 (2005) 2986–2992.
[9] H. Onizuka, M. Kato, T. Shimura, W. Sakamoto, T. Yogo, J. Sol–Gel Sci. Technol. 46 (2008) 107–115.
[10] A. Bozkurt, W. H. Meyer, J. Gutmann, G. Wegner, Solid State Ionics, 164 (2003) 169-176.
[11] O. Acar, U. Sen, A. Bozkurt, A. Ata, Inter. J. Hydro. Energy 34 (2009) 2724-2730.
[12] B. Bingol, W. H. Meyer, M. Wagner, G. Wegner, Macromol. Rapid Commun. 27 (2006) 1719–1724.
[13] H. Niida, M. Takahashi, T. Uchino, T. Yoko, J. Ceram. Soc. Jpn. 111 (2003) 171–175; M. Takahashi, H. Niida, Y. Tokuda, T. Yoko, J. Non-Cryst. Solids 326 & 327 (2003) 524–528; H. Niida, M. Takahashi, T. Uchino, T. Yoko, J. Non-Cryst. Solids 306 (2002) 292–299; M. Megumi, M. Takahashi, Y. Tokuda, T. Yoko, 18 (2006)2075–2080; Y. Tokuda, Y. Tanaka, M. Takahashi, R. Ihara, T. Yoko, J. Ceram. Soc. Jpn. 117 (2009) 842–846.
[14] Y. Tokuda, S. Oku, T. Yamada, M. Takahashi, T. Yoko, H. Kitagawa, Y. Ueda, J. Mater. Res. 26 (2011) 796–803.
[15] M. Takahashi, T. Maeda, K. Uemura, J. Yao, T. Tokuda, T. Yoko, H. Kaji, A. Marcelli, P. Innocenzi, Adv. Mater. 19 (2007) 4343-4346.
[16] Y. K. Kim, L. Gu, T. E. Bryan, J. R. Kim, L. Chen, Y. Liu, J. C. Yoon, L. Breschi, D. H. Pashley, F. R. Tay, Biomaterials 31 (2010) 6618–6627.
[17] A. Aslan, S. Ü. Çelik, A. Bozkurt, Solid State Ionics 180 (2009) 1240–1245.
[18] E. Pretsch, P. Bühlmann, C. Affolter, Determination of Organic Compounds, Springer, Berlin, 2000.
[19] C. J. Pouchert, The Aldrich Library of Infrared Spectra, Aldrich Chemical Company, Wisconsin, 1981.
[20]Yomei Tokuda, Satoshi Nishioka, Yoshikatsu Ueda, Hideki Koyanaka, Hirokazu Masai, Masahide Takahashi, and Toshinobu Yoko, International conference on solid state ionics 18, 2011, Porland

Table 1 Sample notation and composition

notation	composition in molar ratio (VPA : EMA : TTIP)
VET	95 : 50 : 5
VET-ht	95 : 50 : 5 ＊ **heat-treated**
VE	100 : 50 : 0
PVPA	150 : 0 : 0

Table 2 Normalized area of the peaks in ^{31}P MAS NMR spectra of hybrid membranes

structure	chemical shift / ppm	area ratio / %			
		VET	VET-ht	VE	PVPA
T^{0}*	38.0~30.0	35.8	22.9	80.4	82.4
T^{1}*(P)	26.0~23.0	2.7	18.6	0.1	8.7
T^{0}	17.0	51.5	46.5	19.5	8.9
T^{1}(Ti)	12.2	10.1	12.1	—	—

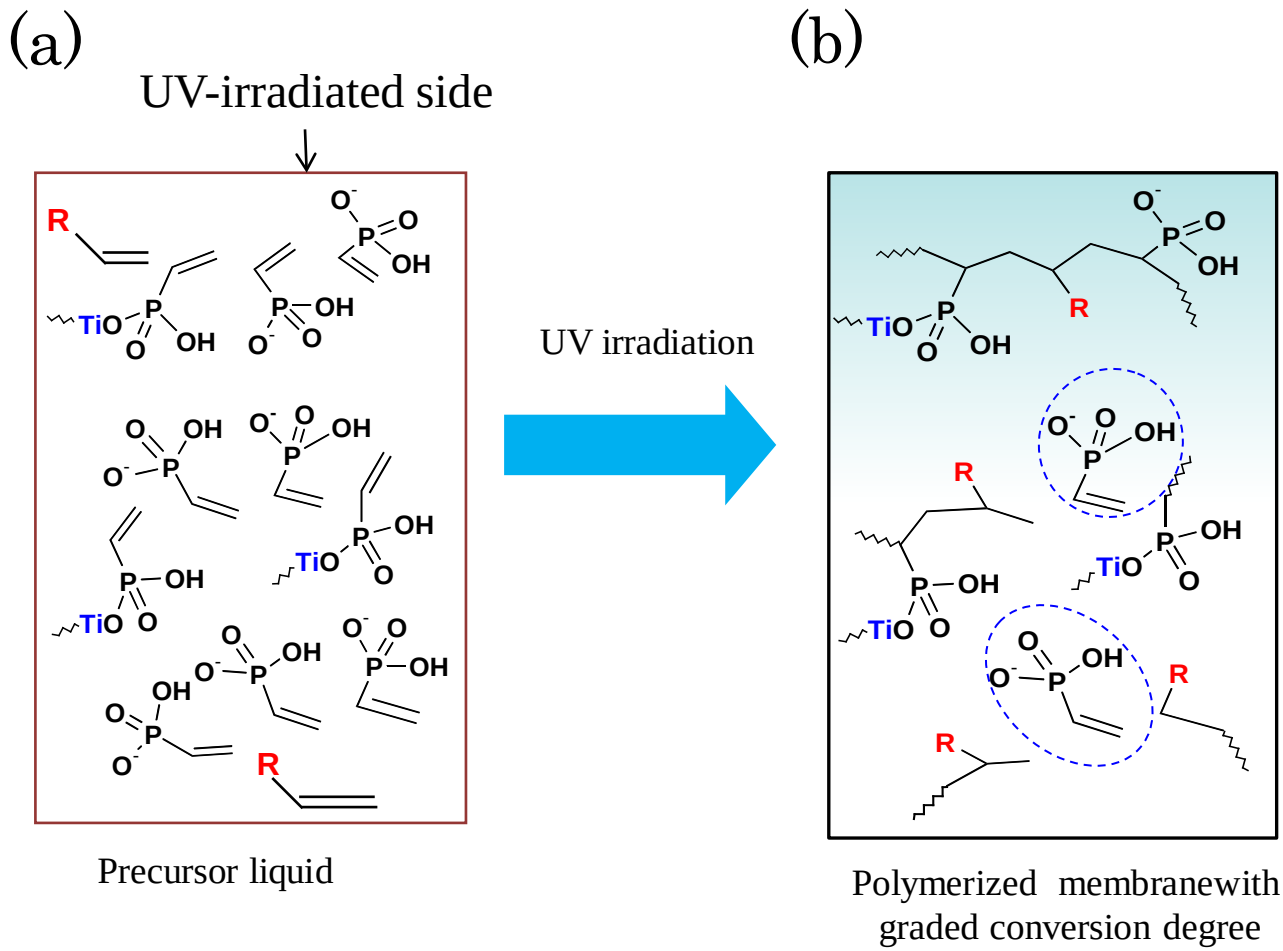

Fig. 1 Schematic representation of membrane with graded degrees of polymerization:
(a) titanophosphite precursor
(b) copolymerized membrane with graded degrees of polymerization

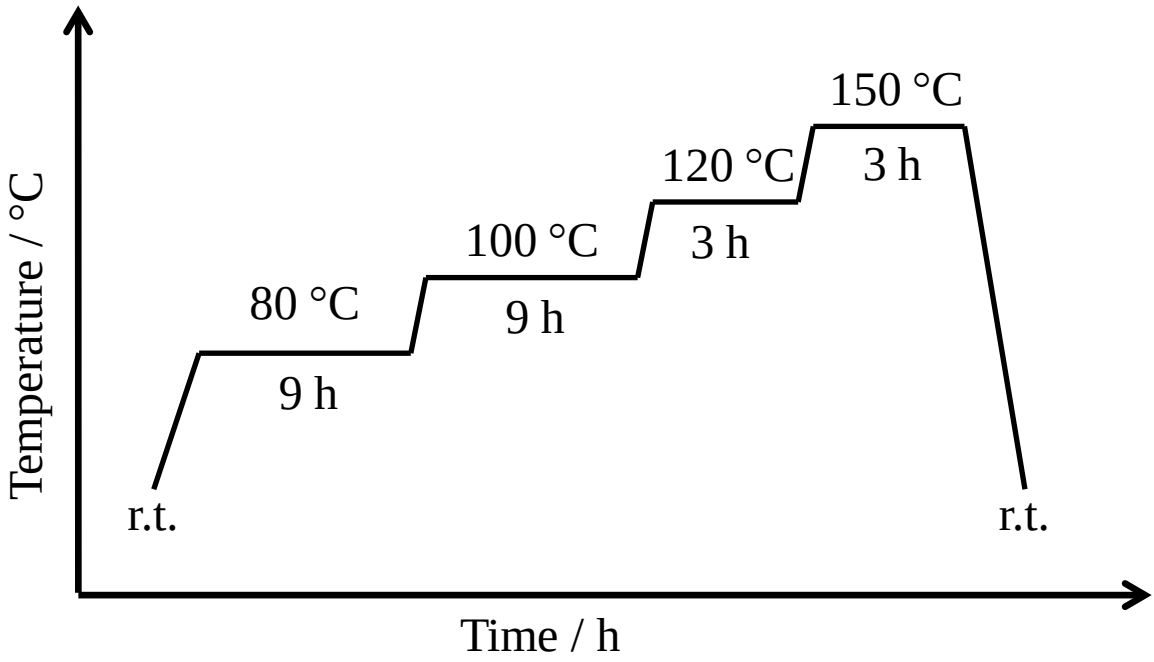

Fig. 2 Temperature program of heat-treatment

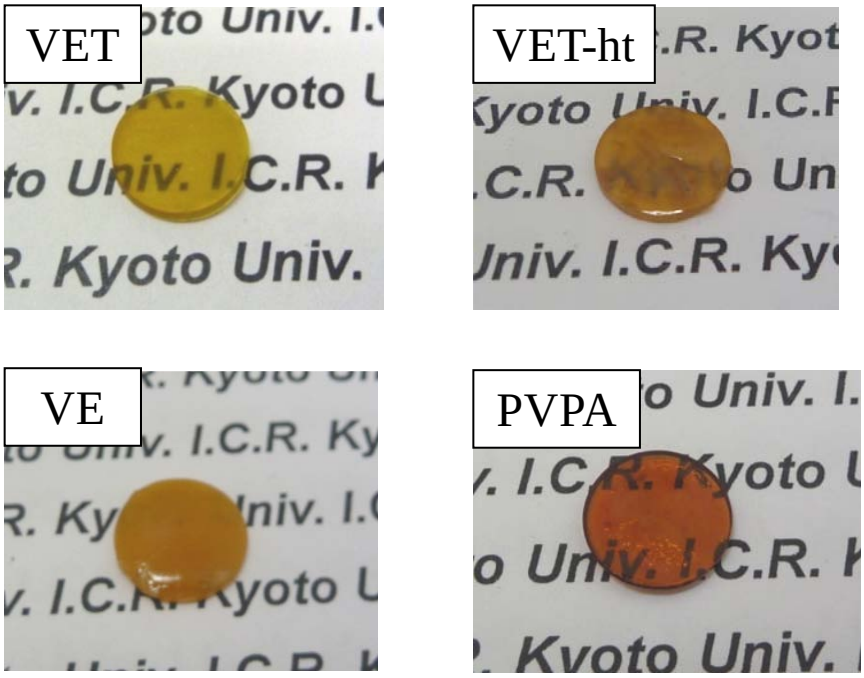

Fig. 3 Photographs of samples prepared

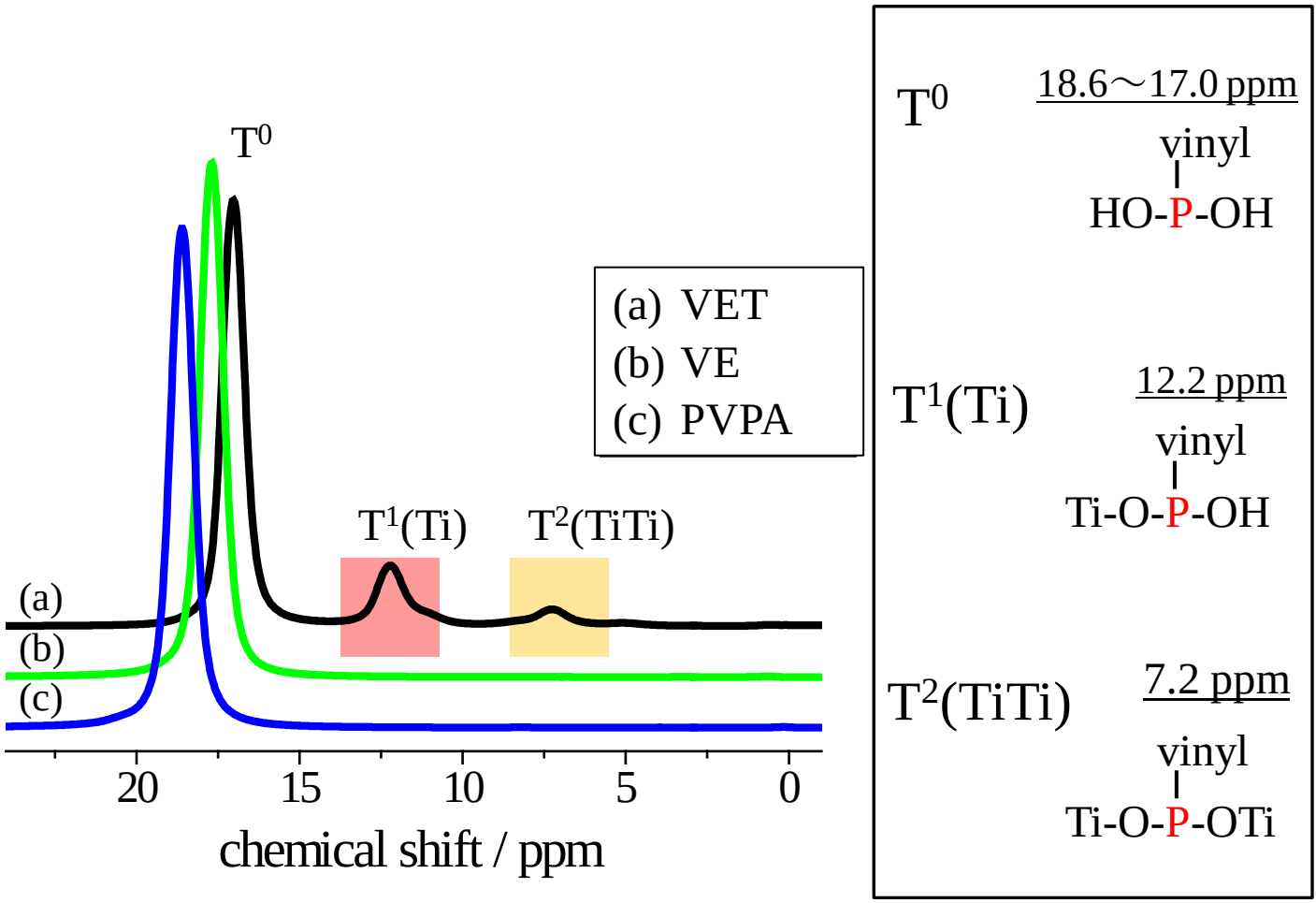

Fig. 4 ^{31}P NMR spectra of VET, VE and PVPA precursor solutions

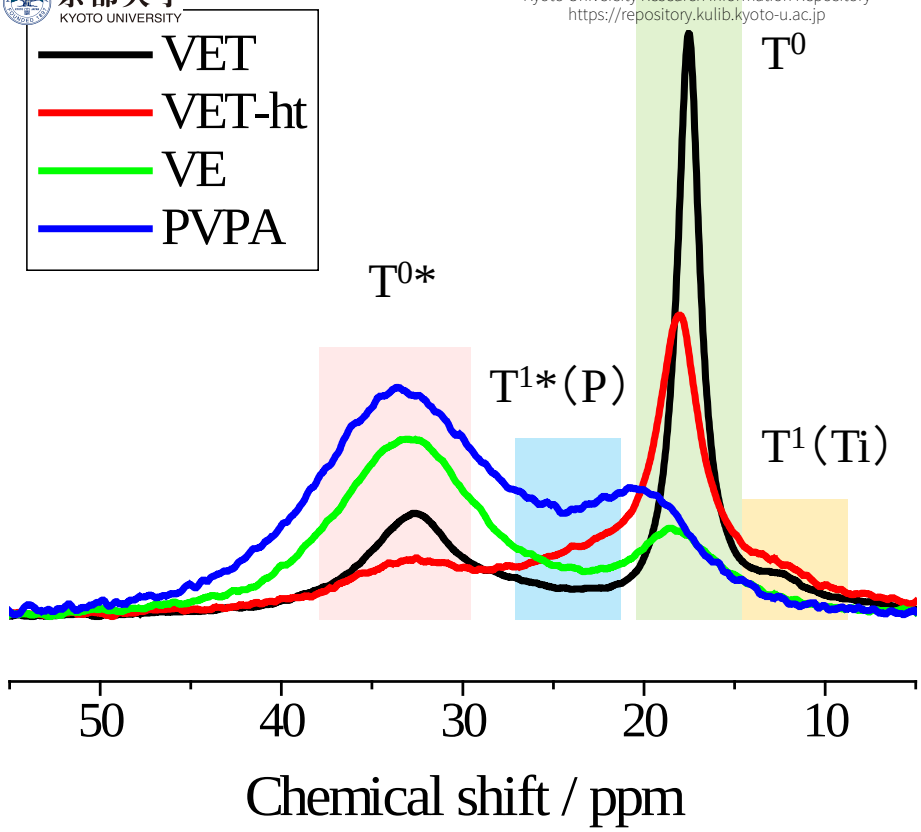

T0*	polymer | HO-P-OH
T1*(P)	polymer | HO-P-O-P
T0	vinyl | HO-P-OH
T1(Ti)	vinyl | Ti-O-P-OH

Fig. 5 ^{31}P MAS NMR spectra of various hybrid membranes

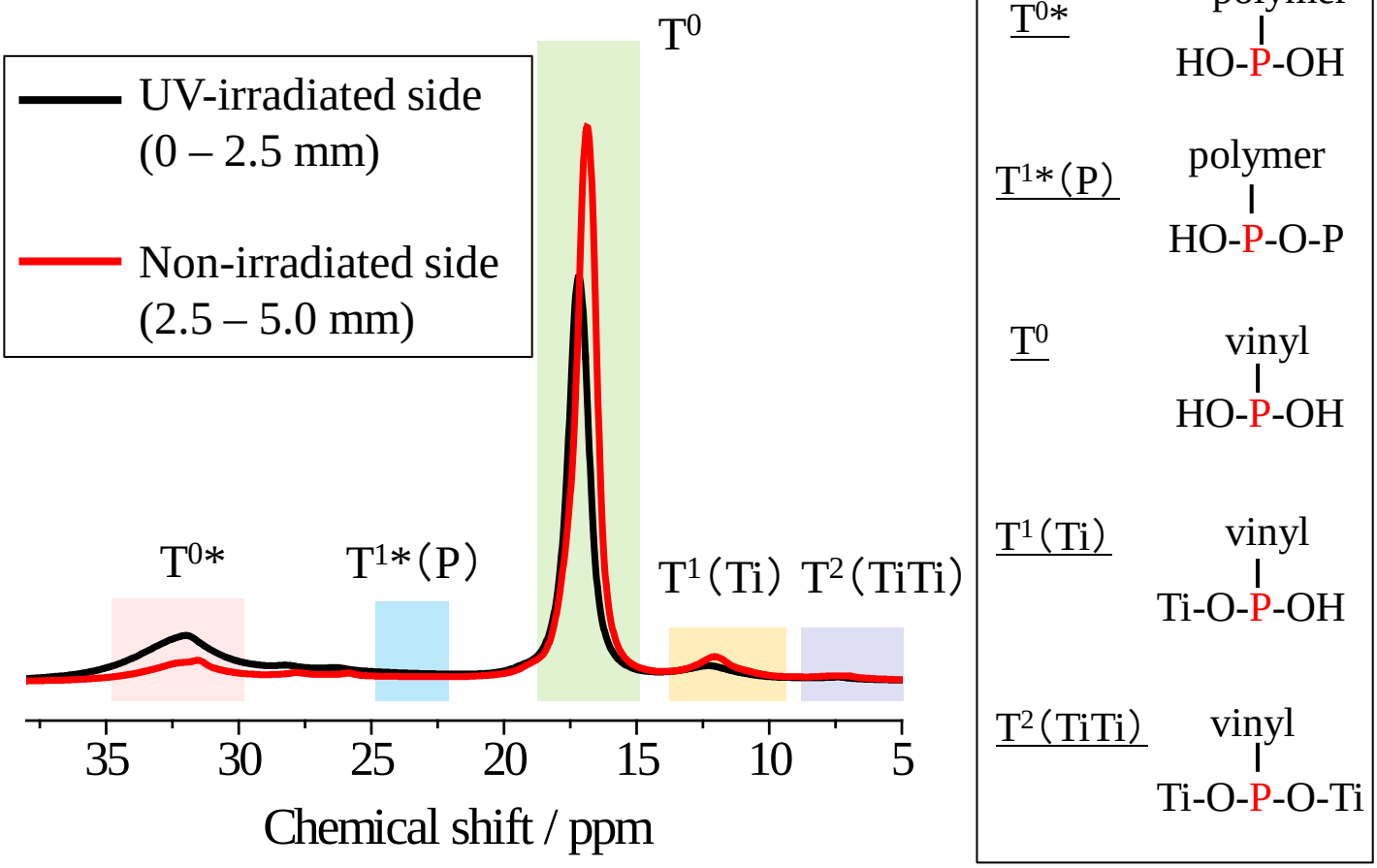

Fig. 6 ^{31}P MAS NMR spectra of thick VET membrane. Black and red lines indicate the spectra of UV-irradiated side and non-irradiated side, respectively.

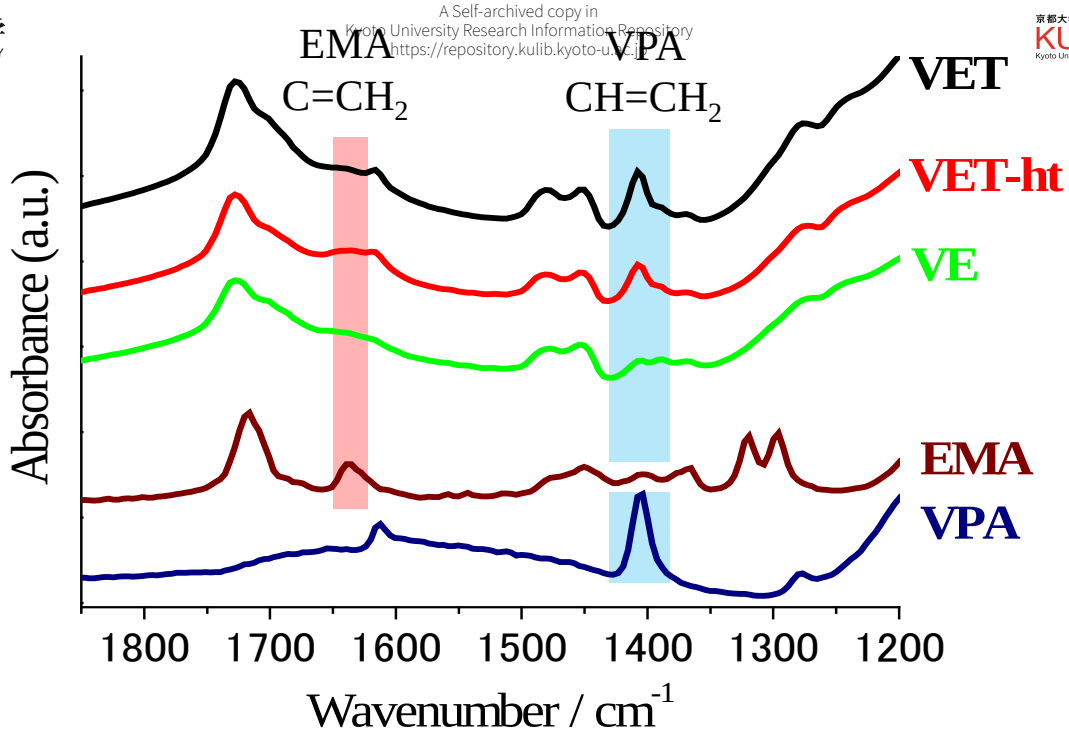

Fig. 7 FT-IR spectra of several hybrid membranes (VET, VET-ht, VE)

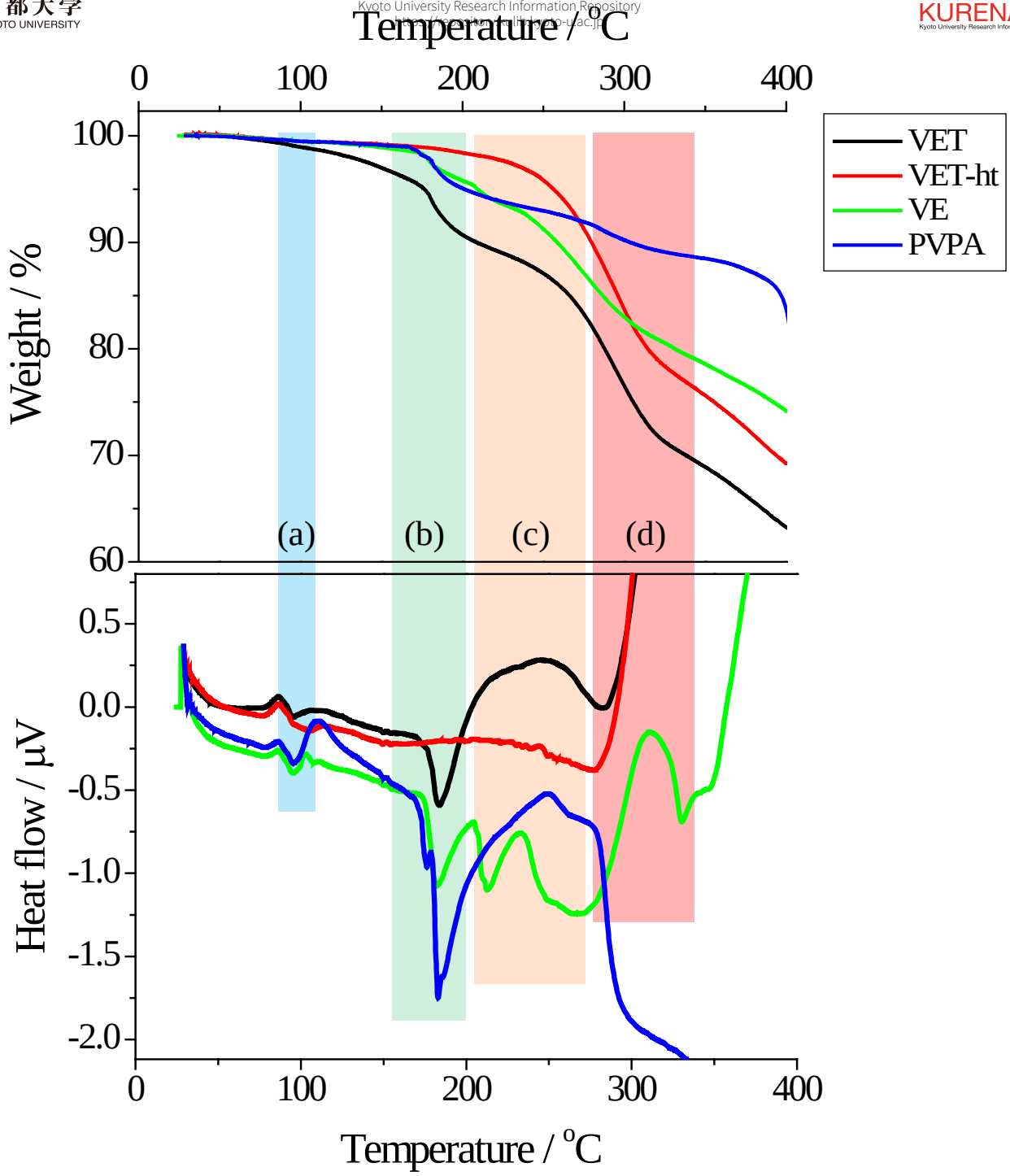

(a) : H_2O ↑
(b) : H_2O ↑ in network
(c) : P-OH condensation
(d) : burn-out of carbonaceous compound

Fig. 8 TG-DTA curves of various hybrid membranes

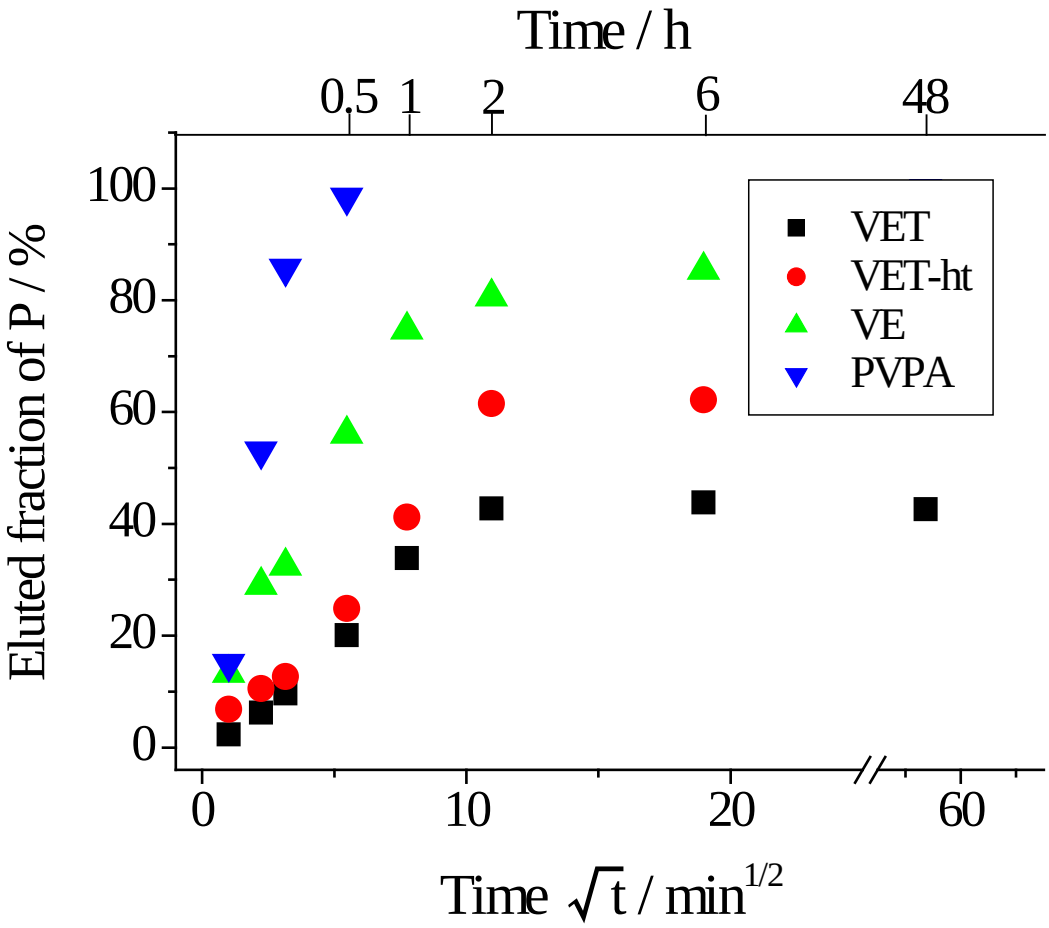

Fig. 9 Time dependence of the eluted P measured by ICP optical emission spectrometry

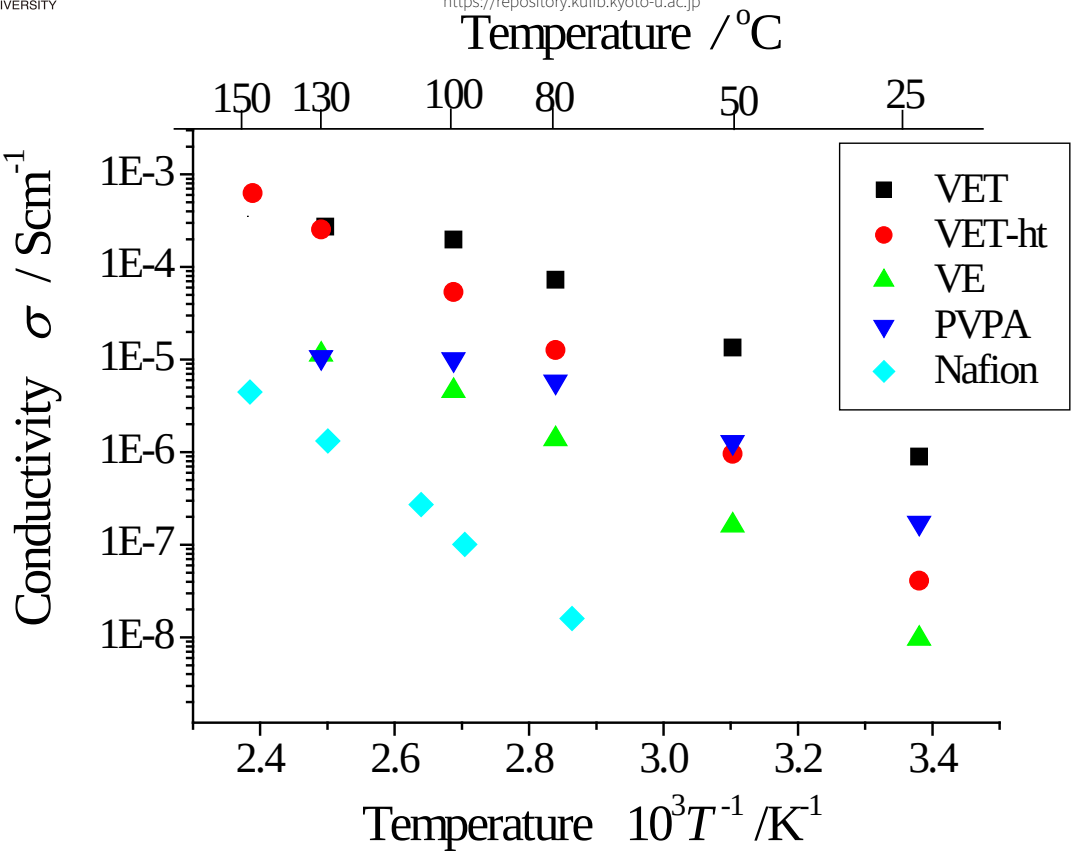

Fig. 10 Temperature dependence of proton conductivity measured without humidification